IMEDITEC 2017

ORIGINAL PAPER

Effect of Cement Line Shielding on the Stress Distribution in Single Osteon with Different Haversian Canal Diameters and Lacunae

A.A. Ismail[a] *, R. Daud[a], , A.K. Junoh[b], N.A.M. Zain[b], M.I. Omar[a]

[a] Fracture and Damage Mechanic Research Group, School of Mechatronic Engineering, Pauh Putra Campus, Universiti Malaysia Perlis (UniMAP), 02600 Arau, Perlis, Malaysia

[b] Institute of Engineering Mathematics Universiti Malaysia Perlis (UniMAP), Kampus Pauh Putra, 02600 Arau, Perlis , Malaysia.

* Corresponding author: aanisayuniismail@gmail.com

INTRODUCTION

Bone has a complex arrangement of structures at multiple scales which contributes to its ability to function as a mechanical support in vertebrae. Its hierarchical structure lead the bone to have high stiffness and strength. Cortical bone and trabecular bone are the main types of bone. Cortical bone is a compact bone that forms the outer layer of the bone that contributes to the bone stiffness and strength. Trabecullar bone is a porous bone that fills the inner spaces of the bones which responsible for body load distribution.

At nanoscale, basic building block of bone is made up of mineralized collagen fibrils. Organic matrix (mostly collagen type I), hydroxyapatite (a calcium phosphate mineral) and water are the three major components that made up the bone At sub-microscale, mineralized collagen fibrils assemble into sheet-like structures which known as lamella (approximately 3-7 µm). In between the lamellae interphase, there is hollow known as lacuna, which host the osteocyte. At microscale, different way of lamellae assembly give rise to trabecular bone and cortical bone (Cowin, 2001; Li *et al*., 2013).

In trabecular bone, the lamellae in the form rods or struts assemble into trabeculae, which form and resorb during bone remodeling, while interstitial bone presence at interconnect of trabeculae. In cortical bone, the lamellae are arranged into concentric cylinder to form osteons (approximately 200 µm - 300 µm in diameter and several milimeters long) which aligned along bone's long axis. At the center of each osteon contains canal, which known as Haversian canal, that host the blood vessels. There is structure fills in between the osteon known as interstitial bone, which consists of remains of old osteon (remnant of primary osteon after bone remodelling).

Interstitial bone has a higher degree of minerelization, but the lamellar structure is similar to the osteon. Each osteon is encircled in cement line to separate it from interstitial bone (boundary of secondary osteon), noted that the primary osteon do not have cement line (Cowin, 2001; Sabet *et al*., 2016). Fig. 1 (a) shows the transverse section of bovine cortical bone which consist of osteon, interstitail bone, cement line and Haversian canal (Budyn *et al*., 2012). The cortical bone microstucture is reported to influence the microcrack propagation path by affecting the maximal stress distribution (Abdel-wahab *et al*., 2012).

Many experiments and computational models have been proposed to predict the mechanical properties of bone at these different structural levels. Past studies have shown that the microstructure of the bone gives the advantage to the bone to resist fracture. Osteon is identified to act as a crack barrier in bone, but in some cases the crack strong enough and able to propagate through the osteon. This causing the osteon to act as a weak point in the bone (Brien *et al*., 2005). Apart from that, the presence of cement line that surrounding the osteon is shown to provide weak path for crack propagation in the bone (Abdel-wahab *et al*., 2012). The cement line was also found to halt the crack from propagating into the osteon (Mischinski & Ural, 2013; Vergani *et al*., 2014). However, the role of cement line in affecting stress distribution in osteon still remain unclear. The hollow structure of the bone, such as lacuna and Haversian canal, are identified as potential stress riser in the bone (Nicolella *et al*., 2005). A study found that the circumferential ellipse-shape lacuna is more advantageous than radial elliptical lacuna and circular lacuna in resist the microdamage (Liu *et al*., 2017). A report suggested that lacunae and other blood vessel channel in bone may increase the bone toughness by slow down the spread of microcrack (Currey, 1962).

Regardless of all the speciality that made up the bone microstructure, cortical bone is still susceptible to fracture. Bone fracture can be caused by various events, such as traumatic falls and sports injuries. Then, it is necessary to align and secure the fractured bone in relatively stable to each other to ensure bone can regenerate in correct orientation and fuse the fracture site. In orthopedic surgical procedures, the bone fracture will be held together by using the internal or external fixator, which consists of screw and plate.

The surgical implementation of implants in attempts to repair the fractured bone itself however can actually lead to introduction of microcrack in the bone structure (see Fig. 1 (b)). This can cause the bone to take longer time to heal or it is possible for the bone to refracture. Multiple studies have been done to investigate the interaction of microcrack with the bone microstructure at many level (Abdel-wahab *et al*., 2012; Budyn & Hoc, 2007; Najafi *et al*., 2007a, 2007b). However, the link between damage at multiscale and whole bone fracture is still absent.

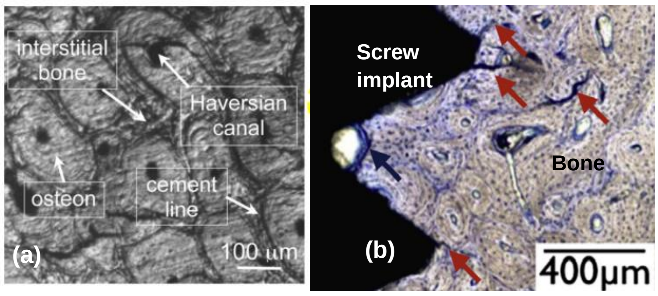

Fig. 1 (a) Optical micrographs of V-threaded implants placed surgically in bone. Red arrows show micro-cracks at bone microstructure, where the yield strength of bone has been exceeded due to high stress concentration from the implant (Coelho & Jimbo, 2014), (b) Light microscopy of a transverse section of cortical bone (Budyn *et al*., 2012)

OPEN ACCESS Freely available online
eISBN 978-967-0194-93-6 FBME

Therefore, this study aims to evaluate the effect of the bone microstructure on the maximum stress distribution in single osteon, which essential for interaction behaviour of bone microstrutures with the microcrack created via the implant stress transfer to cortical bone. In the response of the applied load, the yield stress is expected to concentrated near the natural stress riser, such as lacuna and Haversian canal, in the bone. The interaction between lacunae and lacunae, or between lacuna and Haversian canal are analysed based on the presence of cement line and different Haversian canal diameter.

FINITE ELEMENT MODELING

The micro-structural of osteon is simulated using two models: homogenized and two-phase composite. The homogenous model only consider the osteon, while the two-phase composite consider the osteon and cemenet line. The dimension of lacuna was set to 5 µm × 2 µm (length × width). According to Cowin (2001), the diameter of single osteon ranges from 100 to 300 µm. The geometry of the model was adapted from Giner et al. (2014), which include 10 lacunae in their model which based on feature by Prendergast & Huiskes (1996). Based on these geometry of osteon from the literature, this study simulated the model as a homogenous single osteon with varies number of lacuna and diameter of Haversian canal which explained in detail below. The mechanical properties of the model in

Table 1 was adopted from Abdel-wahab *et al*. (2012).

Table 1 Young's Modulus and Poisson's ratio of cortical bone in transverse direction

Model	Young's Modulus (GPa)	Poisson's ratio
Osteon	9.13	0.17
Cement line	6.85	0.146

Meshing and boundary conditions

The element type used in the simulation was plane 183 solid elements in plain strain condition, as shown in Fig. 3. The simulation was conducted with developed macro codes using ANSYS Mechanical APDL version 14.5 software. Type of meshing element was set as 8-node quadrilateral. The simulations were performed in displacement control mode by constraining the translation along the line on x-axis and translation on y-axis was set at a node in the center of canal. The applied compressive radial loading $\sigma_{r\theta=60^o}$ during this simulation was set to 10 MPa and the load was distributed along the 60º of the arc of osteon (see Fig. 2), following the numerical procedures are done by Giner *et al*. (2014). Evaluation of stress distribution in the model was based on maximum von-Mises stress, $\sigma_{e,max}$.

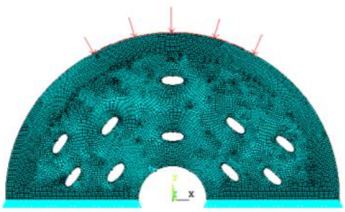

Fig. 2 Model of semi osteon, loading (red arrow along 60º arc of osteon) and boundary condition

Osteon with different canal diameter and cement line

The osteon models are simulated with the presence of 10 lacunae. The width for the osteon was 54.4 µm and width for cement line was 3 µm. The center of the osteon was left empty, which resemble the presence of Haversian canal. The diameter of the canal d_c was set to three different lengths: 20 µm, 30 µm and 40 µm. Hence, the total radius for each osteon model without cement line were 64.4 µm, 69.4 µm and 74.4 µm, respectively, while the total radius for each osteon model with cement line were 67.4 µm, 72.4 µm and 77.4 µm, respectively. Due to the symmetric structure, the model was displayed as semi osteon as shown in Fig. 3.

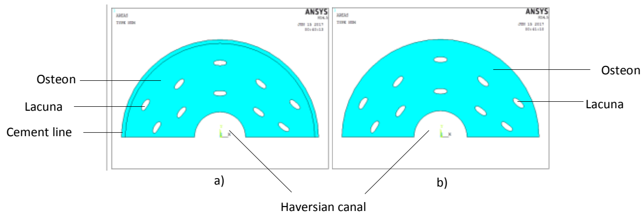

Fig. 3 Model of semi osteon (a) Osteon with the presence of cement line (b) Osteon without cement line.

Osteon with different lacuna distribution and different canal diameter

The osteon models were simulated with different lacunae distribution (6 lacunae, 8 lacunae and 10 lacunae). The lacunae location in all model were fixed. The width for the osteon was 54.4 µm. The center of the osteon was left empty, which resemble the presence of Haversian canal. The diameter of the canal was set to three different diameters: 20 µm, 30 µm and 40 µm. Hence, the total radius for each osteon model were 64.4 µm, 69.4 µm and 74.4 µm, respectively.

RESULTS AND DISCUSSION

Stress distribution in osteon with different canal diameter and presence of cement line

Stress distribution in the osteon models is depicted in Fig. 4. In Fig. 4 (a) and Fig. 4 (d), where the Haversian canal diameter was set to 20 µm, the maximum stress $\sigma_{e,max}$ was seen to yield near the lacuna that was located nearest to the applied loading.

OPEN ACCESS Freely available online
eISBN 978-967-0194-93-6 FBME

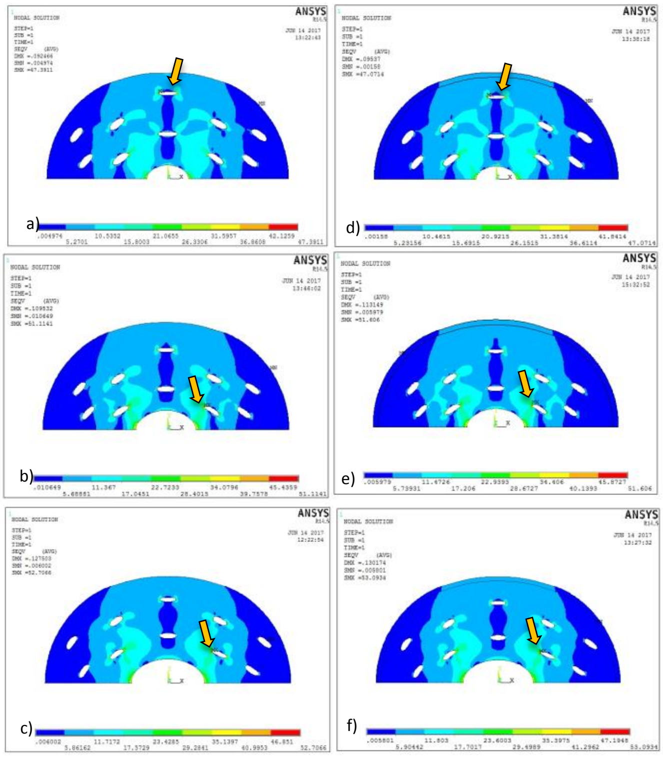

Fig. 4 Stress distribution in single osteon. Fig. 4 (a), Fig. 4 (b) and Fig. 4 (c) show osteon without cement line, d_c = 20 µm, 30 µm and 40 µm respectively, while Fig. 4 (d), Fig. 4 (e) and Fig. 4 (f) show osteon with cement line, d_c= 20 µm, 30 µm and 40 µm respectively.The arrow point to the $\sigma_{e,max}$.

In Fig. 4 (b) and Fig. 4 (e), where the Haversian canal was set to 30 µm, the $\sigma_{e,max}$ was seen to yield near the lacuna near the Haversian canal. This result was same in the model with d_c = 40 µm in Fig. 4 (c) and Fig. 4 (f), the $\sigma_{e,max}$ was seen at the edge of lacuna near the canal. Qualitatively, the $\sigma_{e,max}$ in both model (model with cement lines and without cement line) were yield at the same location. Fig. 5 shows the increase of $\sigma_{e,max}$ as the canal diameter increase from and the presence of cement line. However, the $\sigma_{e,max}$ value in the osteon with cement line and without cement line were approximately similar in osteon with canal diameter 20 µm, while the maximum stress was slightly different in osteons with canal dimeter 30 µm and 40 µm. The $\sigma_{e,max}$ was lowest in models with Haversian canal set to 20 µm, followed by the models with d_c = 30 µm and the highest $\sigma_{e,max}$ in models with d_c = 40 µm. This results correlated with the literature that stated the canal could act as the stress riser *(*Nicolella *et al.*, 2005). The precense of cement line seems not affecting the maximum stress in the models. But, the cement line do play a role in deflecting the crack from entering the osteon (Mischinski & Ural, 2013; Vergani *et al*., 2014). Apart from that, as discussed earlier, the maximum stress in osteon with d_c = 20 µm was located at the edge of lacuna nearest to the given load, the stress may concentrated at the lacuna and shield the osteon from higher stress.

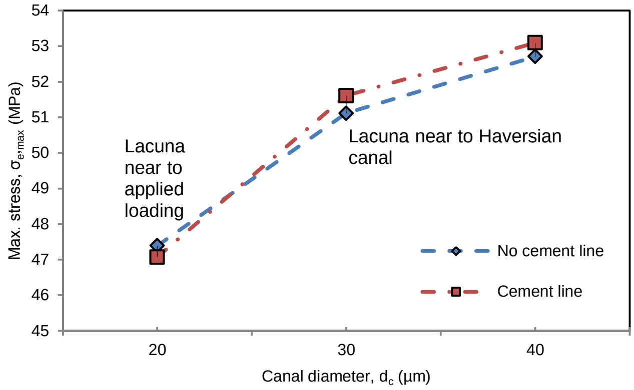

Fig. 5 Maximum stress aginst the diameter of Haversian canal in model with cement line and in model with no cement line.

Stress distribution in osteon with different lacuna distribution and different canal diameter

Stress distribution in osteon models with three different lacunae distribution and different canal diameter are shown in Fig. 6(a)-(i). Fig. 6(a), Fig. 6(b), Fig. 6(c) are the models with Haversian canal d_c = 20 µm with number of lacunae 6, 8 and 10 respectively. In these three osteon models with d_c = 20 µm, it is shown that the stress were yielded at the edge of lacuna that located near to the applied load. Then, Fig. 6(d), Fig. 6(e), Fig. 6(f) are the models with d_c = 30 µm with number of lacunae 6, 8 and 10 respectively. The stresses were also concentrated at the edge of the lacuna near the applied load in models only for lacunae distribution 6 and 8. The lacunae distribution 10 was observed with the maximum stress concentrated at the lacuna near to the Haversian canal. Next, Fig. 6(g), Fig. 6(h), Fig. 6 (i) are the models with d_c = 40 µm with number of lacunae 6, 8 and 10 respectively. In these three models, the maximum stress area were at different lacunae. The maximum stress was noted at the lacuna near the applied load in model with 6 lacunae, while in models with 8 and 10 lacunae, the maximum stress was seen to concentrate at the lacuna nearest to the Haversian canal. In these three models, the maximum stress area were at different lacunae. The maximum stress was noted at the lacuna near the applied load in model with 6 lacunae, while in models with 8 and 10 lacunae, the maximum stress was seen to concentrate at the lacuna nearest to the Haversian canal. The quantiatative value of maximum stresses were plotted in the graph shown in Fig. 7.

OPEN ACCESS Freely available online
eISBN 978-967-0194-93-6 FBME

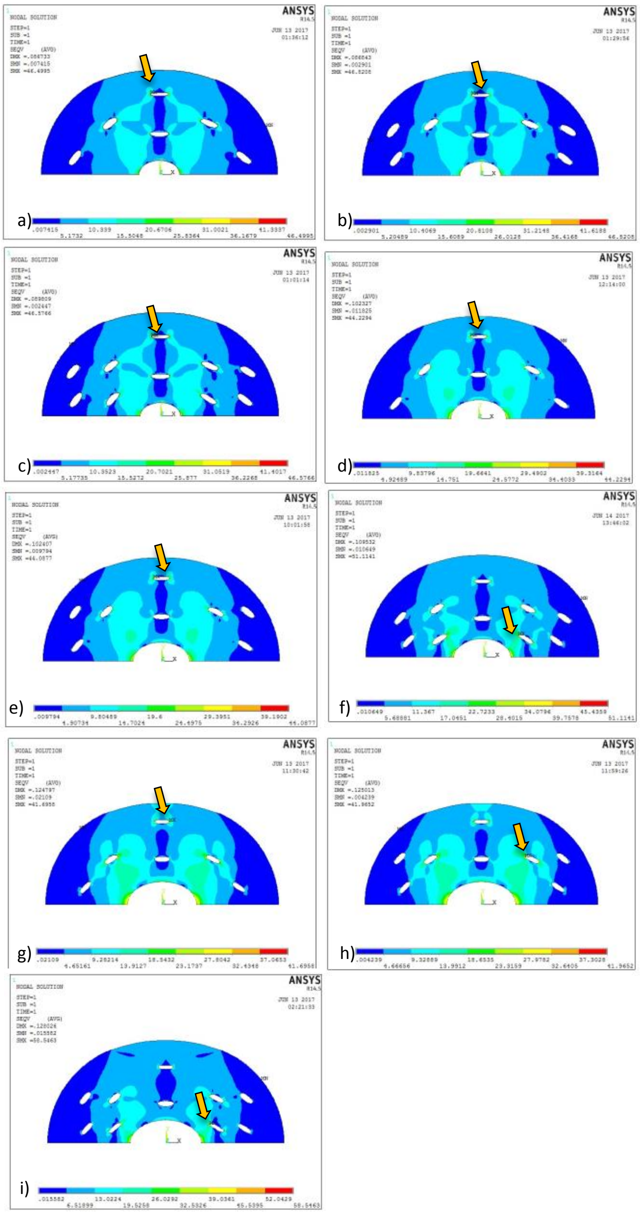

Fig. 6 Stress distribution in single osteon. Fig. 6(a), Fig. 6(b), Fig.6(c) are the osteons with Haversian canal diameter d_c= 20 µm, and Fig. 6(d), Fig. 6(e), Fig. 6(f) are the osteon with d_c= 30 µm, Fig. 6 g), Fig. 6 h), Fig. 6(i) are the osteons with d_c = 40 µm with number of lacunae 6, 8 and 10 respectively. The arrow point to the $\sigma_{e,max}$.

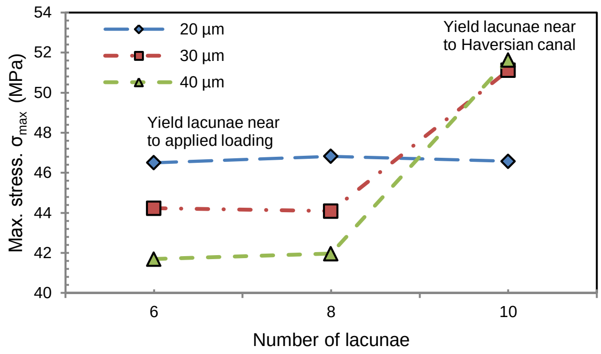

Fig. 7 Maximum stress aginst the number of lacunae in model with different Haversian canal diameter (20 µm, 30 µm and 40 µm)

In the graph shows the maximum stress in models with Haversian canal d_c = 20 µm with different lacuna distribution did not showing much different. But, the maximum stress in these models (smaller canal diameter) were the highest compared to the other models with different Haversian canal diameter. The maximum stress was lowest in model with d_c = 40 µm with 6 lacunae and 8 lacunae, followed by model with canal diameter set to 30 µm with 6 and 8 lacunae. However, the magnitude of maximum stress increase tremendously in model with d_c =30 µm and 40 µm with the presence of 10 lacunae. Apart from that, it is noted that the area of maximum stress in the models were not fixed, except in models with canal diameter 20 µm where the maximum stress located at the lacuna nearest to the applied load. In model that have 10 lacunae with d_c = 30 µm and 40 µm, the maximum stress was shown concentrated at the lacuna nearest to the canal, and the magnitude of the stress was shown to increase drastically compare if the $\sigma_{e,max}$ located at the lacuna near the applied load.

CONCLUSION

Bone is known for its unique structure that give it the ability to take heavy stress. This paper has successfully analysed the stress distribution in the microstructure of cortical bone using FE modeling. The cortical anatomical model of single osteon is considered to investigate the stress shielding distribution affected by different geometry of microtructure. The different Haversian canal diameter d_c were shown to affect the magnitude of $\sigma_{e,max}$ in the model. The bigger the canal diameter, the higher the maximum stress yield in the model (constant lacunae number). It can be concluded that if $d_c \leq 20$ µm, the yield lacunae are concentrated to the nearest applied loading while for $d_c > 20$ µm, the yield lacunae are concentrated to the nearest Haversial canal. The presence of cement line seems do not affect the maximum stress for $d_c \leq 20$ µm but gradually affect the stress concetration as $d_c > 20$ µm. Based on lacunae distribution, for all 6,8 and 10 lacunae, the yielded lacunae for $d_c \leq 20$ µm were located near to applied compressive radial loading $\sigma_{r\theta=60^o}$. As $d_c > 20$ µm, at d_c = 30 µm and d_c = 40 µm, the increase of lacunae quantity has promoted stress yielding at lacunae near to Haversian canal.

ACKNOWLEDGEMENT

OPEN ACCESS Freely available online
eISBN 978-967-0194-93-6 FBME

The authors are very grateful for the research support of Ministry of Higher Education (MoHE) Malaysia and Universiti Malaysia Perlis through awarded Fundamental Research Grant (FRGS 9003-00578).

REFERENCES

Abdel-wahab, A. A., Maligno, A. R., & Silberschmidt, V. V. (2012). Micro-scale modelling of bovine cortical bone fracture : Analysis of crack propagation and microstructure using X-FEM. *Computational Materials Science*, *52*(1), 128–135.

Brien, F. J. O., Taylor, D., & Lee, T. C. (2005). The effect of bone microstructure on the initiation and growth of microcracks, *23*.

Budyn, É., & Hoc, T. (2007). Multiple scale modeling for cortical bone fracture in tension using X-FEM.

Budyn, E., Jonvaux, J., Funfschilling, C., & Hoc, T. (2012). Bovine Cortical Bone Stiffness and Local Strain are Affected by Mineralization and Morphology. *Journal of Applied Mechanics*, *79*(January 2012), 1–12.

Coelho, P. G., & Jimbo, R. (2014). Osseointegration of metallic devices : Current trends based on implant hardware design. *Archives of Biochemistry and Biophysics*, *561*, 99–108.

Cowin, S. (2001). *Bone Mechanics Handbook* (Second Edi). CRC Press.

Currey, J. D. (1962). Stress concentrations in bone. *Quarterly Journal of Microscopical Science*, *103*(1), 111–133.

Giner, E., Arango, C., Vercher, A., & Fuenmayor, F. J. (2014). Numerical modelling of the mechanical behaviour of an osteon with microcracks. *Journal of the Mechanical Behavior of Biomedical Materials*, *37*, 109–124.

Li, S., Abdel-wahab, A., & Silberschmidt, V. V. (2013). Analysis of fracture processes in cortical bone tissue. *Engineering Fracture Mechanics*, *110*, 448–458.

Liu, Y., Chen, B., Yin, D., & Chen, B. (2017). Effects of direction and shape of osteocyte lacunae on resisting impact and micro-damage of osteon. *Journal of Materials Science: Materials in Medicine*, 1–7.

Mischinski, S., & Ural, A. (2013). Interaction of microstructure and microcrack growth in cortical bone : a finite element study, *16*(1), 81–94.

Najafi, A. R., Arshi, A. R., Eslami, M. R., Fariborz, S., & Moeinzadeh, M. (2007a). Haversian cortical bone model with many radial microcracks : An elastic analytic solution, *29*, 708–717.

Najafi, A. R., Arshi, A. R., Eslami, M. R., Fariborz, S., & Moeinzadeh, M. H. (2007b). Micromechanics fracture in osteonal cortical bone : A study of the interactions between microcrack propagation , microstructure and the material properties, *40*, 2788–2795.

Nicolella, D. P., Bonewald, L. F., & Moravits, D. E. (2005). Measurement of microstructural strain in cortical bone. *Eur J Morphol*, *42*(1–2), 23–29.

Prendergast, J., & Huiskes, R. (1996). Microdamage and Osteocyte- Lacuna Strain in Bone : A Microstructural Finite Element Analysis. *Journal of Biological Chemistry*, *118*(May), 240–246.

Sabet, F. A., Najafi, A. R., Hamed, E., & Jasiuk, I. (2016). Modelling of bone fracture and strength at different length scales : a review, 20–30.

Vergani, L., Colombo, C., & Libonati, F. (2014). Crack propagation in cortical bone : a numerical study. *Procedia Materials Science*, *3*, 1524–1529.

OPEN ACCESS Freely available online
eISBN 978-967-0194-93-6 FBME